AGU PUBLICATIONS

Earth and Space Science

RESEARCH ARTICLE
10.1002/2015EA000143

Key Points:
- OCO 2 X_{CO2} retrieval fails to pass the internal quality check over desert regions
- We explain the physical mechanism of retrieval degeneracy over a surface near critical albedo
- Over a surface near the critical value, the X_{CO2} retrieval loses accuracy

Correspondence to:
Q. Zhang,
qzh@caltech.edu

Citation:
Zhang, Q., R.-L. Shia, S. P. Sander, and Y. L. Yung (2016), X_{CO2} retrieval error over deserts near critical surface albedo, *Earth and Space Science*, *3*, doi:10.1002/2015EA000143.

Received 21 OCT 2015
Accepted 28 DEC 2015
Accepted article online 3 JAN 2016

X_{CO2} retrieval error over deserts near critical surface albedo

Qiong Zhang[1], Run-Lie Shia[1], Stanley P. Sander[2], and Yuk L. Yung[1]

[1]Division of Geological and Planetary Sciences, California Institute of Technology, Pasadena, California, USA, [2]Jet Propulsion Laboratory, California Institute of Technology, Pasadena, California, USA

Abstract Large retrieval errors in column-weighted CO_2 mixing ratio (X_{CO2}) over deserts are evident in the Orbiting Carbon Observatory 2 version 7 L2 products. We argue that these errors are caused by the surface albedo being close to a critical surface albedo (α_c). Over a surface with albedo close to α_c, increasing the aerosol optical depth (AOD) does not change the continuum radiance. The spectral signature caused by changing the AOD is identical to that caused by changing the absorbing gas column. The degeneracy in the retrievals of AOD and X_{CO2} results in a loss of degrees of freedom and information content. We employ a two-stream-exact single scattering radiative transfer model to study the physical mechanism of X_{CO2} retrieval error over a surface with albedo close to α_c. Based on retrieval tests over surfaces with different albedos, we conclude that over a surface with albedo close to α_c, the X_{CO2} retrieval suffers from a significant loss of accuracy. We recommend a bias correction approach that has significantly improved the X_{CO2} retrieval from the California Laboratory for Atmospheric Remote Sensing data in the presence of aerosol loading.

1. Introduction

The Orbiting Carbon Observatory 2 (OCO 2) mission was launched in July 2014 to measure the concentration of CO_2 accurately from space. OCO 2 was designed to map the global column-averaged CO_2 dry air mixing ratio (X_{CO2}) in order to characterize CO_2 sources and sinks on regional scales [*Kuang et al.*, 2002; *Crisp et al.*, 2004]. The OCO 2 instrument features high precision, small footprint, and global coverage. It is ideal for studying the global carbon cycle. Since CO_2 is well mixed in the atmosphere, CO_2 flux inversion typically requires retrieval accuracy up to 1 ppm [*Miller et al.*, 2007]. Such data could significantly reduce the uncertainties in the regional CO_2 flux estimation [*Rayner and O'Brien*, 2001]. However, any X_{CO2} retrieval errors larger than the accuracy requirement would lead to significant biases in the flux inversion.

Aerosol scattering is often considered the major source of error in the remote sensing of greenhouse gases [*Aben et al.*, 2007]. Scattering in the atmosphere could change the photon path distribution, thus altering the apparent absorption of the target trace gas [*Oshchepkov et al.*, 2008]. There are many recent studies on the CO_2 retrieval errors related to aerosol scattering. For example, *Houweling et al.* [2005] examined the Scanning Imaging Absorption Spectrometer for Atmospheric Chartography CO_2 retrieval and found a bias of up to 10% over the Sahara Desert. *Uchino et al.* [2012] compared the Greenhouse Gases Observing Satellite retrievals with Total Carbon Column Observing Network and lidar measurements over Tsukuba and identified high-altitude aerosols and thin cirrus clouds as the major sources of error.

The surface albedo has often the most significant effect on the reflected radiance observed at top of atmosphere even in the presence of aerosol scattering. The concept of critical surface albedo (α_c) was first proposed by *Fraser and Kaufman* [1985]. Intuitively, increasing aerosol optical depth (AOD) could either increase or decrease the top of atmosphere reflectance as the aerosols appear to be brighter (such as sulfate) or darker (such as soot) than the surface. The critical surface albedo is defined as the albedo where the derivative of the top of atmosphere radiance with respect to AOD is equal to zero in the continuum [*Seidel and Popp*, 2012]. In the continuum, clear-sky gaseous absorption optical depth is zero. A surface with albedo close to α_c could cause large errors in the retrieval of AOD from space, since the radiance measurement loses sensitivity to the variation of AOD. The concept of critical surface albedo has been extensively applied in the retrieval of surface and aerosol properties [e.g., *Banks et al.*, 2013; *Sayer et al.*, 2013]. However, it is less well known in the field of greenhouse gas retrieval. While aerosols are hard to detect over a surface with albedo close to α_c, they can change the photon path length and therefore influence the retrieval of greenhouse gas column abundances.

The aim of this paper is to test the hypothesis that the OCO 2 X_{CO2} retrieval errors over desert regions are due to the albedo being close to the critical surface albedo. In section 2, we examine the OCO 2 version 7 data to

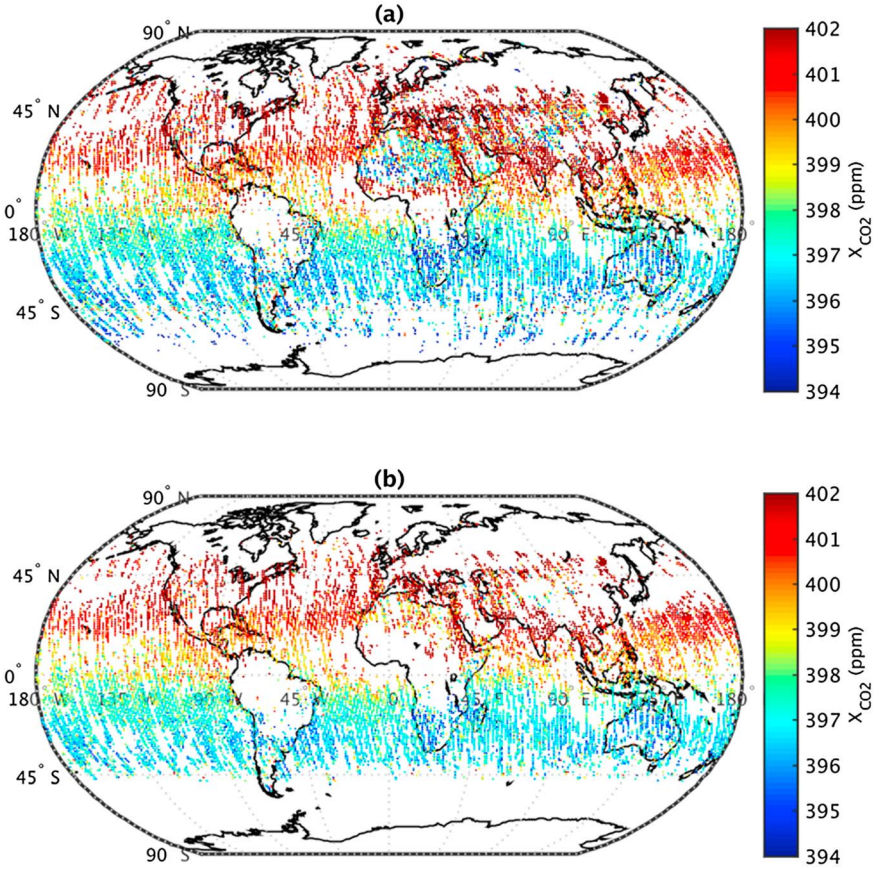

Figure 1. Global map of OCO 2 X_{CO2} retrieval in April 2015. (a) All the data points are displayed. In OCO 2 retrievals, data qualities are labeled with flags 0 and 1: 0, passed internal quality check; 1, failed internal quality check. (b) Only the data points labeled with "flag 0" are displayed.

identify regions with large X_{CO2} retrieval errors. In section 3, we employ a two-stream-exact single scattering (2S-ESS) radiative transfer model to study the physical mechanism of the X_{CO2} retrieval errors over a surface with albedo close to α_c. A discussion of our results follows in section 4.

2. X_{CO2} Retrieval Errors Over Deserts

In this section, we study the OCO 2 retrieval error over desert regions where surface albedos are high. Online Version 7 data are used in the study (http://oco.jpl.nasa.gov/science/ocodatacenter/). In the OCO 2 data set, retrieval quality is labeled with two "flags": 0, "passed internal quality check"; 1, "failed internal quality check. In Figure 1, we plot all the X_{CO2} retrievals in April 2015. Currently, OCO 2 gathers as many as 72,000 spectra on the sunlit side of any single orbit or 24 per second [*Mandrake et al.*, 2013]. Monthly data are enough for global coverage. By comparing Figures 1a and 1b, we find that most of the data points that fail to pass the quality check are located over desert regions such as the Sahara Desert and central Asia. X_{CO2} retrievals over these regions show significant low biases compared with surrounding areas. Since the deserts are unlikely to be a significant sink of CO_2, X_{CO2} retrieval bias over these regions appears to be an artifact.

We will examine the hypothesis that the retrieval errors over desert regions are due to the albedo being close to the critical surface albedo. The concept of critical surface albedo is explained in Figure 2. The three panels represent (a) clear scenario, (b) scattering over a low albedo surface, and (c) scattering over a surface with albedo close to α_c. Schematic figures of one-line spectra are also shown in each panel. Intuitively, bright aerosols over a dark surface would increase the radiance in the continuum, as shown in Figure 2b. The presence of such aerosols is very easy to detect from the shift of the continuum radiance. However, over a critical surface albedo region, as shown in Figure 2c, increasing the AOD does not change the absolute radiance in

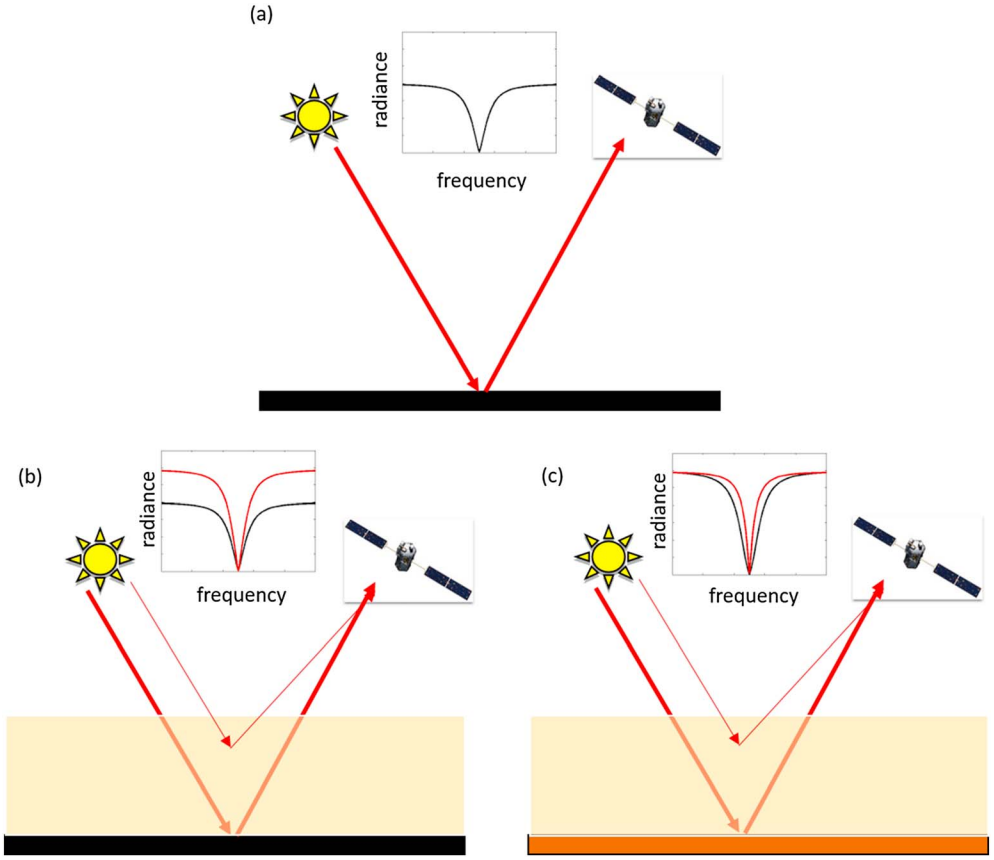

Figure 2. Schematic figures of reflection and scattering over surfaces with difference albedos. The small window at the top of each panel shows the one-line absorption spectra. Black spectra represent the reflection in a clear scenario over a dark surface. Red spectra represent the reflection and scattering in a hazy scenario. (a) Clear scenario, AOD = 0. (b) Scattering over a dark surface. (c) Scattering over a surface with albedo close to α_c.

the continuum. Aerosols can cause changes in the photon path length through the atmosphere, thereby modifying the apparent absorption. The net result is the filling-in of the absorption lines, while the continuum remains the same. We will demonstrate in the next section that over such a surface with albedo close to α_c, the effect of changing AOD is almost the same as that caused by changing absorbing gas column abundance. Over such regions, the interference between aerosol scattering and CO_2 absorption will cause degeneracy in the retrieval of AOD and CO_2, leading to a large error in the X_{CO2} retrieval.

To confirm our hypothesis that the retrieval errors are caused by the surface albedo being close to the critical value, we examine the surface albedo in Figure 3. Figure 3a shows the retrieved surface albedo in the CO_2 1.6 μm weak band, and Figure 3b shows the difference between the retrieved surface albedo and the critical surface albedo of 0.46, a value that is estimated in the next section using the 2S-ESS model. In the calculation of the critical surface albedo, we assume that the aerosol has mineral dust properties over the desert with single scattering albedo (SSA) = 0.94 [*Kahn et al.*, 2005]. The critical surface albedo corresponding to mineral dust is much higher than the ocean albedo and is also higher than land albedos in most areas. Figure 3 shows that the only areas with such high albedos are deserts, where the X_{CO2} retrieval errors are large.

It is well known that AOD can be large over desert regions due to wind and dust [*Houweling et al.*, 2005]. We plot the total AOD and the retrieved mineral dust AOD from the OCO 2 product in Figure 4. AOD values are shown in the O_2 0.76 μm absorption band. Over the deserts, we suspect that the AOD retrieval is biased. Since mineral dust aerosol acts to change the photon path length [*Houweling et al.*, 2005], the CO_2 column abundance retrieval would also be biased, as shown in Figure 1. There are several reasons that lead us to attribute the X_{CO2} retrieval errors to the interaction between AOD and critical surface albedo, instead of the large AOD alone.

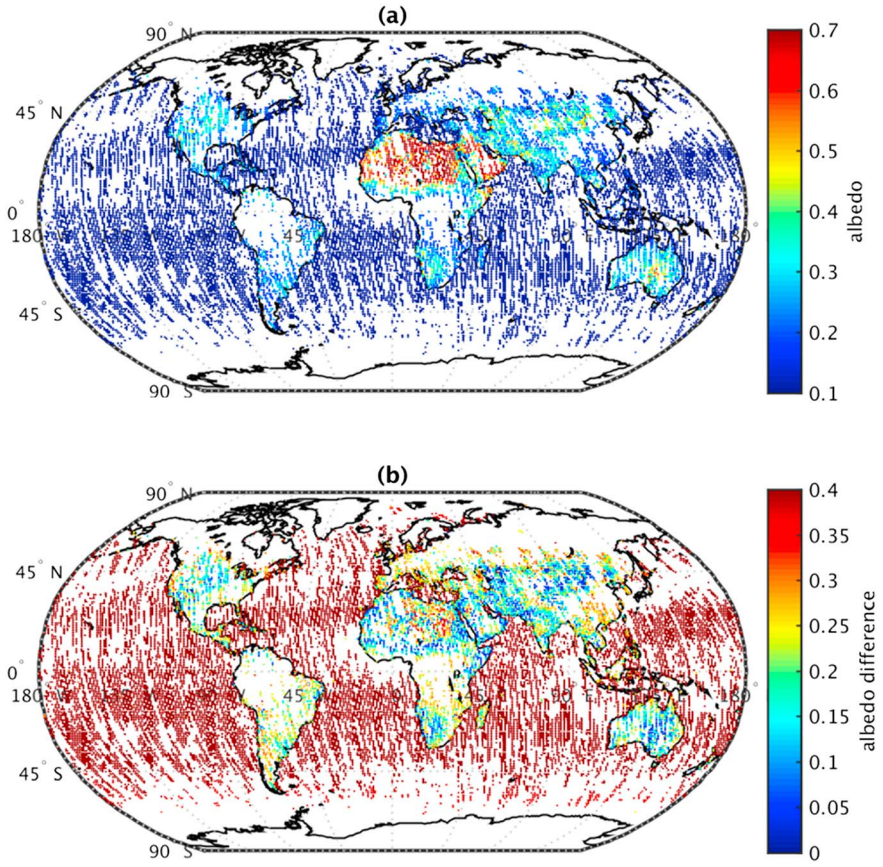

Figure 3. (a) Global map of the retrieved surface albedo in the 1.6 μm weak CO_2 band in April 2015. (b) Difference between the retrieved surface albedo and the critical surface albedo of 0.46. Differences are displayed in absolute values. We assume that the aerosol has mineral dust properties with SSA = 0.94. In section 3, we use the same surface albedo for all the absorption bands in the simulations.

1. Desert is not the only region with high aerosol loadings. Over other regions with high pollution levels and large AOD, such as megacities in the eastern U.S. and China, the X_{CO2} retrievals have much lower biases than those over desert regions.
2. Due to atmospheric circulation, dust aerosol over the Sahara Desert extends far into the Atlantic Ocean, as seen in the Moderate Resolution Imaging Spectroradiometer (MODIS) product [see *Houweling et al.*, 2005, Figure 1b; *Remer et al.*, 2008, Figure 8]. However, in Figures 1 and 4, we see a clear contrast in the X_{CO2} and AOD retrievals between the ocean and the land on the boundary of the African continent. The X_{CO2} retrieval differences between the land and the adjacent ocean are most evident near the Sahara Desert. We assume that such differences in the OCO 2 product are unrealistic, although ocean retrievals are done using glint mode and land retrievals using nadir mode.
3. We examine the regions in Figure 1b where the X_{CO2} retrieval fails to pass the quality check or shows a low bias and the regions in Figure 3b where the surface albedo is very close to the critical surface albedo relevant to mineral dust. The two regions coincide to a large extent.

3. Radiative Transfer Modeling

The concept of critical surface albedo can be explained by a numerically efficient 2S-ESS radiative transfer model [*Spurr and Natraj*, 2011]. This model is better than a traditional numerical two-stream model in that the singly scattered radiation is computed exactly, while the two-stream approximation is used only for the multiply scattered radiation. It has been used in several previous studies on the remote sensing of greenhouse gases [e.g., *Xi et al.*, 2015; *Zhang et al.*, 2015]. We use a typical model atmosphere derived from the National Centers for Environmental Prediction-National Center for Atmospheric Research reanalysis data

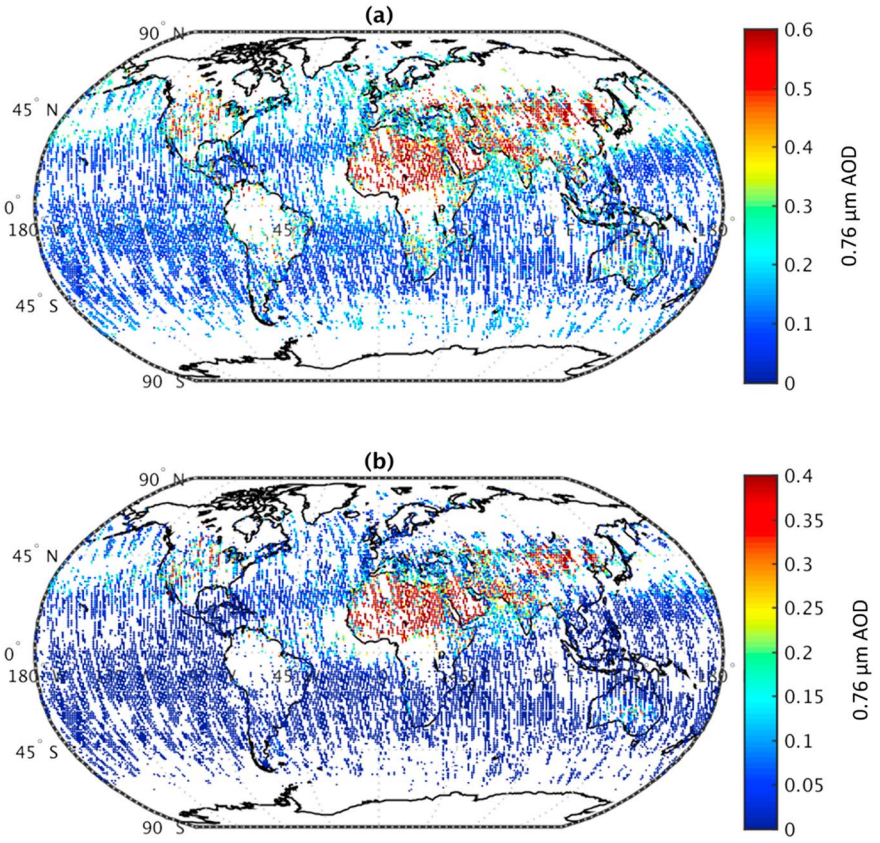

Figure 4. (a) Global map of the OCO 2 total AOD retrieval in April 2015. AOD values are shown in the O_2 0.76 μm absorption band. (b) Same as Figure 4a but for "type 1" aerosol in the OCO 2 retrieval [*O'Dell et al.*, 2012], i.e., mineral dust [*Kahn et al.*, 2005].

[*Kalnay et al.*, 1996]. The. model atmosphere includes 70 layers from the surface to the top of atmosphere. Absorption coefficients for all absorbing gases are obtained from the HITRAN database [*Rothman et al.*, 2009]. Rayleigh scattering is included in the calculation. To simulate OCO 2 nadir observations in the midlatitude, we assume that the viewing zenith angle is zero, while the solar zenith angle is set to 45°. The incoming solar flux is assumed to be unity for all wavelengths (we effectively calculate the dimensionless reflectance). Aerosol scattering in this model is isotropic. The AOD is distributed evenly within the boundary layer below 800 hPa. The isotropic scattering assumption is equivalent to the Delta-Eddington approximation of a more realistic forward-peaked dust aerosol phase function [*Wiscombe*, 1977]. This assumption has minor impact on the accuracy of radiative transfer calculation and does not influence the conclusions in this study with respect to surface albedo and SSA. Figures 5a–5c show the simulated spectra in the 2.0 μm strong CO_2 band, 1.6 μm weak CO_2 band, and 0.76 μm O_2-A band. Water vapor absorption is not included in this model.

Intuitively, increasing AOD in the atmosphere will change the continuum radiance since aerosol scattering changes the apparent albedo. We assume that the aerosol SSA is fixed for mineral dust; however, the surface albedo may vary widely across different regions. Figure 5b shows the variation of the AOD Jacobian (derivative of radiance with respect to AOD) in the continuum of the 1.6 μm weak CO_2 band as a function of surface albedo. Mineral dust aerosol increases the apparent albedo over a dark surface and decreases the apparent albedo over a bright surface. Of interest, then, is the transition point at which the derivative of the radiance with respect to AOD changes sign (equation (1)). In Figure 5b, this point is marked by the dotted red line ($\alpha_c = 0.46$). Mathematically we can derive it as follows:

$$\frac{\partial R(\mathrm{AOD}, \alpha_c)}{\partial \mathrm{AOD}} = 0 \tag{1}$$

Equation (1) can be solved numerically using a radiative transfer model. As shown in *Seidel and Popp* [2012], α_c is primarily a function of aerosol SSA. Aerosols with larger SSA correspond to larger critical surface albedo

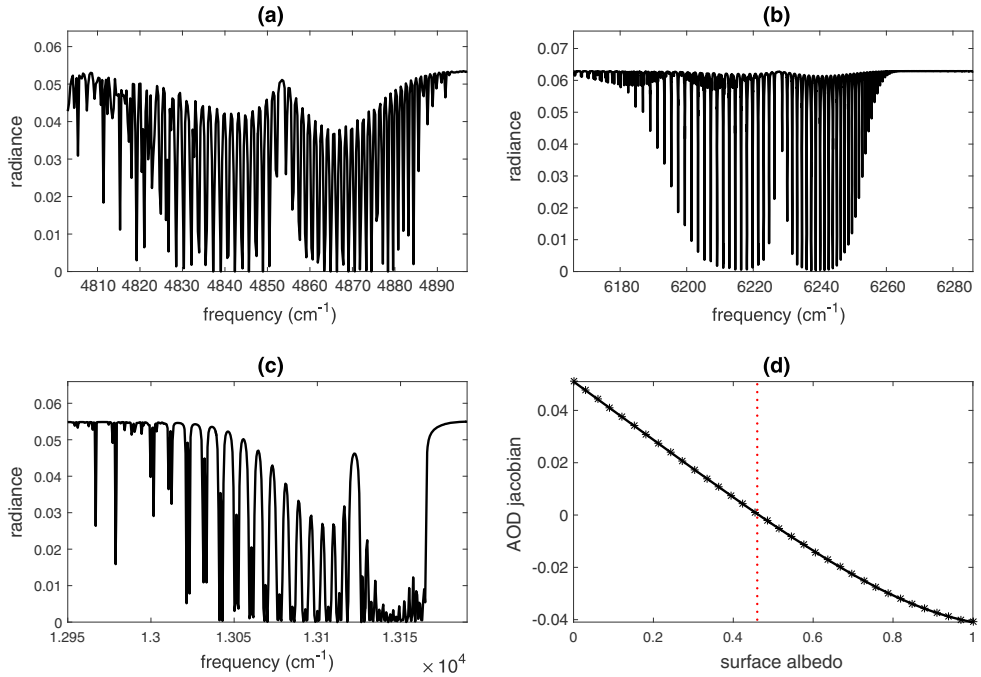

Figure 5. (a) Spectrum of 2.0 μm strong CO_2 band. (b) Spectrum of 1.6 μm weak CO_2 band. (c) Spectrum of 0.76 μm weak O_2-A band. (d) AOD Jacobian in the continuum as a function of surface albedo. The critical surface albedo (0.46) is marked by the red dotted line.

values. In addition, the value of α_c is also associated with many other factors such as viewing geometry and aerosol height distribution.

In an optically thick atmosphere, the value of α_c can be roughly estimated as the reflectance of an infinitely thick atmosphere [*Goody and Yung*, 1989]:

$$\alpha_c = R_{\text{inf}}(\omega_0) = \frac{1-\sqrt{1-\omega_0}}{1+\sqrt{1-\omega_0}} \tag{2}$$

where ω_0 is the aerosol SSA. This is based on the assumption that the incoming solar flux is approximated by an isotropic diffusive flux in the atmosphere. Equation (2) gives a simple analytic relationship between α_c and ω_0. The critical surface albedo is a monotonically increasing function of aerosol SSA, which is consistent with the numerical results in *Seidel and Popp* [2012] and *Wells et al.* [2012]. However, in an optically thin atmosphere, equation (2) would overestimate the value of α_c. In this case, the critical surface albedo needs to be solved numerically using a realistic radiative transfer model.

The aerosol SSA is defined as the ratio between the scattering optical depth and the total extinction optical depth. Within the absorption line, gaseous absorption must be added on to the aerosol extinction optical depth; therefore, the relationship between SSA and critical surface albedo no longer holds. An important implication is that if the surface albedo approaches the critical value, it is difficult to retrieve AOD. In this scenario, the sensitivity of the reflected radiance to AOD will decrease, and retrieval errors for both AOD and CO_2 will increase.

In an atmosphere with both aerosol scattering and gaseous absorption, this relationship for the critical surface albedo only holds in the continuum. Within the absorption line, the derivative of radiance with respect to AOD is not zero. In Figure 6, we zoom in on a single absorption line in the 1.6 μm weak CO_2 band and calculate the Jacobians with respect to AOD and CO_2 total column (scaling factor) over a low albedo surface and a surface with albedo close to α_c. Over a low albedo surface, increasing AOD has two effects: (1) increasing the radiance as the aerosol appears to be brighter than the surface; (2) changing the apparent absorption as the scattering modifies the photon path length. In Figures 6c and 6d, the AOD and CO_2 Jacobians are easy to distinguish. However, over a surface with albedo close to α_c, increasing AOD does not change the radiance in the continuum. In this scenario, the only effect of aerosol scattering is to change the apparent absorption.

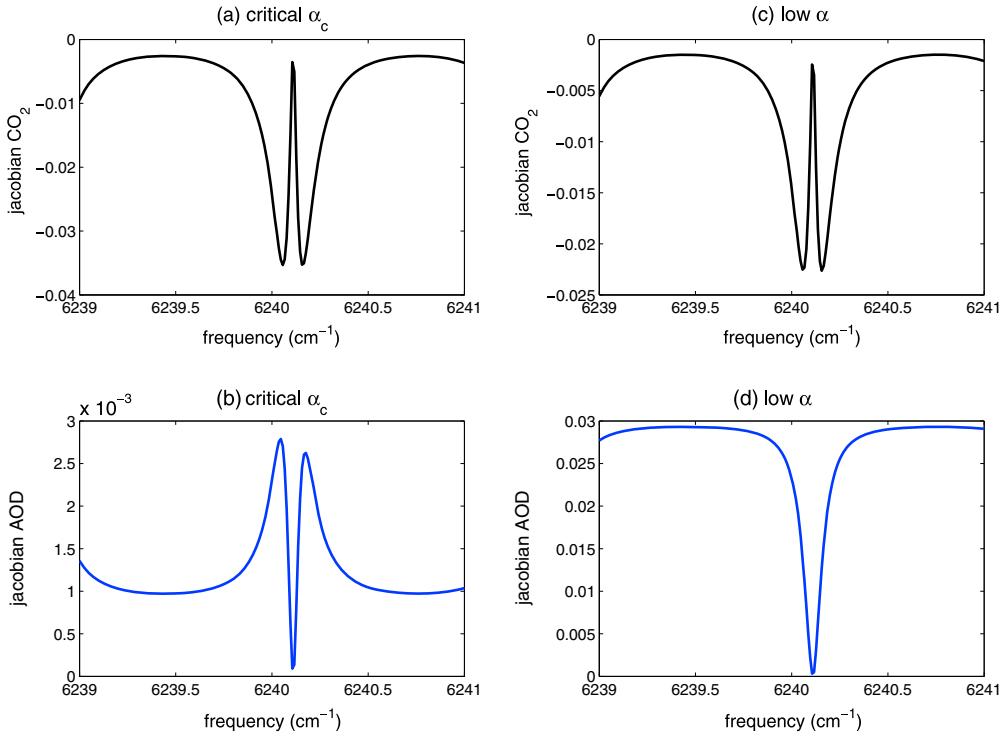

Figure 6. Jacobians of CO_2 and AOD in a single line, generated by the 2S-ESS model. (a) Jacobian of CO_2 total column over a surface with albedo close to α_c (0.46). (b) Jacobian of AOD over a surface with albedo close to α_c (0.46). (c) Same as Figure 6a but over a low albedo (0.2) surface. (d) Same as Figure 6b but over a low albedo (0.2) surface.

Therefore, the AOD and CO_2 Jacobians, as shown in Figures 6a and 6b, respectively, have almost the same shape. At low spectral resolution, the signals from AOD and CO_2 would not be distinguishable in the observations.

Using the 2S-ESS model, we can study the retrieval error caused by the surface albedo being close to the critical value. Here retrieval error is defined as the difference between the retrieved state variables and the truth. It is different from the posterior error, which is computed from the a posteriori covariance and depends only on the measurement noise. OCO 2 uses an optimal estimation approach to retrieve X_{CO2} and other state vector variables [*Rodgers*, 2000] based on minimizing the following cost function:

$$\chi^2 = [\mathbf{x_i} - \mathbf{x_a}]^T \mathbf{S}_a^{-1} [\mathbf{x_i} - \mathbf{x_a}] + [\mathbf{y} - \mathbf{F}(\mathbf{x_i})]^T \mathbf{S}_e^{-1} [\mathbf{y} - \mathbf{F}(\mathbf{x_i})], \tag{3}$$

where $\mathbf{x_i}$ is the state vector, $\mathbf{x_a}$ is the a priori state vector, $\mathbf{F(x)}$ is the forward model, $\mathbf{y}$ is the measurement, $\mathbf{S}_a$ is the a priori covariance matrix, and $\mathbf{S}_e$ is the measurement error covariance matrix.

We use two quantities to determine the retrieval quality and precision: degrees of freedom (d) and information content (H). They are calculated using equations (4)–(5).

$$d = \sum_i \lambda_i{}^2 / \left(1 + \lambda_i{}^2\right), \tag{4}$$

$$H = \frac{1}{2} \ln\left(\left| \left(\mathbf{K^T S_e^{-1} K} + \mathbf{S_a^{-1}} \right) \mathbf{S_a} \right| \right), \tag{5}$$

where $\mathbf{K}$ is the Jacobian matrix with respect to CO_2 and AOD, and $\{\lambda_i\}$ are the singular values of the normalized Jacobian $\mathbf{S}_e^{-\frac{1}{2}} \mathbf{K} \mathbf{S}_a^{\frac{1}{2}}$. Degree of freedom and information content measure, respectively, how many independent pieces of information we can obtain from the measurements and how much the estimation of the state vector can be improved given the information from the measurement.

To simplify the problem, we set up a retrieval scheme assuming that only three state variables are included in the state vector, i.e., total column CO_2 (scaling factor), AOD, and surface pressure. In the calculation, their a priori uncertainties are arbitrarily assumed to be 20%, 100%, and 0.4%, respectively. They are consistent with

Table 1. Retrieval Tests Using the 2S-ESS Model[a]

	X_{CO2} Error	AOD Error	Surface Pressure Error	*d*	*H*
Low albedo (0.2)	0.97	0.0008	−0.41	2.843	11.82
Critical albedo (0.46)	3.22	−0.1018	−6.22	2.565	8.09
High albedo (0.9)	1.09	0.0009	−1.89	2.850	11.12

[a]X_{CO2} errors are in ppm. Surface pressure errors are in hPa. Errors are defined as the difference between the retrieved state variables and the truth (retrieved—truth).

the retrieval algorithm shown in *O'Dell et al.* [2012]. We assume that the three state variables are not correlated. Therefore, the a priori covariance matrix $\mathbf{S}_a$ is diagonal. The Jacobian matrix $\mathbf{K}$ is calculated using finite differences, and the measurement error covariance matrix $\mathbf{S}_e$ is defined according to the signal-to-noise ratio (SNR). We employ the Levenberg-Marquardt algorithm [*Rodgers*, 2000] to minimize the cost function. The iteration in this algorithm is

$$\mathbf{x_{i+1}} = \mathbf{x_i} + \left[(1+\gamma)\mathbf{S}_a^{-1} + \mathbf{K}_i^T\mathbf{S}_e^{-1}\mathbf{K}_i\right]^{-1}\left\{\mathbf{K}_i^T\mathbf{S}_e^{-1}[\mathbf{y} - \mathbf{F}(\mathbf{x_i})] - \mathbf{S}_a^{-1}[\mathbf{x_i} - \mathbf{x_a}]\right\}, \quad (6)$$

where γ is the parameter determining the size of each iteration step. In the retrieval tests, we generate synthetic measurements using the 2S-ESS model within the three absorption bands, as shown in Figures 5a–5c. For simplicity, surface albedo and AOD are the same for all the three bands. We employ a spectral resolution of 0.3 cm^{-1} in the weak and strong CO_2 absorption bands and 0.6 cm^{-1} in the O_2-A band. SNR is set to be 100. Gaussian white noise is added to the synthetic data. The SNR used in the retrieval tests is lower than the OCO 2 instrument SNR [*Frankenberg et al.*, 2015]. In addition to the radiometric noise, it includes other sources of error such as uncertainties in the HITRAN spectroscopic parameters and unresolved solar lines. We assume that the a priori and first guess values of X_{CO2}, AOD, and surface pressure are 380 ppm, 0.3, and 998 hPa, respectively. These values are different from the truth, which are 400 ppm for X_{CO2}, 0.6 for AOD, and 1000 hPa for surface pressure.

Retrieval results for different values of surface albedo are listed in Table 1. We evaluate the error in the retrieved X_{CO2} over three scenarios: a low albedo surface ($\alpha = 0.2$), a surface with albedo close to α_c ($\alpha_c = 0.46$), and a high albedo surface ($\alpha = 0.9$). All parameters are the same for the three cases except for the surface albedo. Over a surface with albedo close to α_c, the retrieval of the three state variables suffers from degeneracy. Further, the errors in the retrieved X_{CO2} can be as large as 3.2 ppm over a surface with albedo close to α_c, while retrieval errors over a high or low albedo surface are about 1 ppm. The large X_{CO2} retrieval error over a surface with albedo close to α_c is related to the inaccurate AOD retrieval, which is mainly due to the loss of degrees of freedom and information content.

4. Discussions and Conclusions

We have analyzed the X_{CO2} retrieval errors over deserts and attributed the errors to the surface albedo being close to the critical value, α_c. It is apparent that such errors, if not taken into account, could cause large biases in the inversion of CO_2 sources and sinks. The 2S-ESS radiative transfer model provides clear insights into the physical mechanism of aerosol scattering over a surface with albedo close to α_c. In this study, the value of α_c is determined in the 1.6 μm weak CO_2 band. Surface albedos in the strong CO_2 band and O_2-A band do not necessarily satisfy the condition of critical surface albedo. Even by using all the three measured bands, we still see a significant increase in the X_{CO2} retrieval error when the surface albedo in the weak CO_2 band is close to α_c. The transition of retrieval error from a low/high surface albedo to the critical surface albedo is a smooth function. There is a significant increase in the retrieval error, and a loss of degrees of freedom, if the surface albedo falls within $\alpha_c \pm 0.1$ (Figure 7). We use a 2S-ESS model in this study because it is simple and can reveal the basic physics of the impact of critical albedo on X_{CO2} retrieval. We plan to explore a more realistic model in future collaborative work with the OCO 2 retrieval team.

In addition to the interaction between aerosol scattering and critical surface albedo, there are many other sources of error in the X_{CO2} retrieval, such as cirrus clouds, uncertainties in the spectroscopic parameters, and large solar zenith angles. In Figure 1, we also identify large retrieval errors in high latitude regions and over South America. However, these errors are probably not related to surface albedo. Retrieval errors over these regions warrant further investigation.

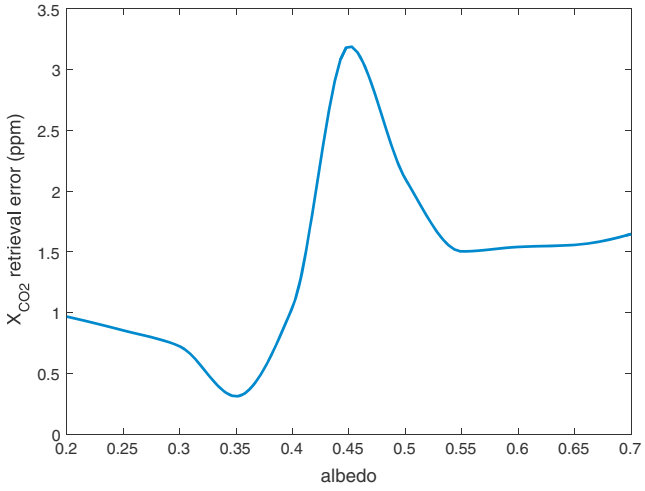

Figure 7. X_{CO2} retrieval error as a function of surface albedo. The same retrieval test as shown in Table 1 has been done at various surface albedos.

The problem over a surface with albedo close to α_c is essentially a degeneracy in the retrieval. Although the magnitude of the AOD Jacobian is small over such a surface, its signal is almost identical to the CO_2 mixing ratio Jacobian, which leads to a loss of degrees of freedom and information content. In this scenario, the information on AOD mainly comes from the a priori, and its retrieval has large smoothing errors. This error in the AOD retrieval will change the photon path length and influence the X_{CO2} retrieval. We have tested synthetic data by retrieving them using the 2S-ESS model. We see a large X_{CO2} error over a surface with albedo close to α_c, when the AOD a priori deviates away from the true value.

To reduce the error, we need to bring in additional information to constrain aerosol properties. If we use more accurate AOD a priori information and apply a stronger a priori constraint, X_{CO2} retrievals over surfaces with albedo close to α_c could be improved. Given the same error in AOD estimation, the X_{CO2} retrieval error over a surface with albedo close to α_c could be even smaller than that over a high or low albedo surface, since the Jacobian of AOD over a surface with albedo close to α_c is smaller. One possible solution is to fix the surface pressure at the European Centre for Medium-Range Weather Forecasts (ECMWF) [*Uppala et al.*, 2005] reanalysis value and retrieve AOD using the O_2 absorption band [*Sanghavi et al.*, 2012]. When the O_2 column abundance is known, aerosol information can be obtained from the O_2 absorption lines. *Zhang et al.* [2015] has proposed a similar solution for the retrieval of X_{CO2} from the California Laboratory for Atmospheric Remote Sensing (CLARS) measurements. Since the ECMWF surface pressure reanalysis data are very accurate [*Ponte and Dorandeu*, 2003], it should be acceptable to fix the surface pressure. Retrieval tests similar to those shown in Table 1 have been done to confirm that aerosol information from the O_2-A band could significantly reduce the X_{CO2} retrieval error over a surface with albedo close to α_c. For OCO 2, we still need an accurate estimate of the Ångström coefficient to translate the AOD in the O_2-A band to a value that is relevant to the weak CO_2 band. Alternatively, information on aerosols and surface albedo from other satellites, such as Multiangle Imaging Spectroradiometer and MODIS [*Kahn et al.*, 2005; *Liang et al.*, 2002], could also be employed to improve OCO 2 retrievals.

Acknowledgments
We thank A. Eldering, M. Gunson, V. Natraj, J. Margolis, S. Newman, and K.-F. Li for their helpful comments. We also thank the Editor, F.C. Seidel, and an anonymous reviewer whose comments helped improve the manuscript significantly. This research was supported in part by NASA grant NNX13AK34G to the California Institute of Technology, a grant from the OCO 2 mission at Jet Propulsion Laboratory, and the KISS program at Caltech. The OCO 2 data used in this study can be downloaded from http://oco.jpl.nasa.gov/science/ocodatacenter/.

References

Aben, I., O. Hasekamp, and W. Hartmann (2007), Uncertainties in the space-based measurements Of CO_2 columns due to scattering in the Earth's atmosphere, *J. Quant. Spectrosc. Radiat. Transfer*, *104*, 450–459.

Banks, J. R., H. E. Brindley, C. Flamant, M. J. Garay, N. C. Hsu, O. V. Kalashnikov, L. Kluser, and A. M. Sayer (2013), Intercomparison of satellite dust retrieval products over the west African Sahara during the Fennec campaign in June 2011, *Remote Sens. Environ.*, *136*, 99–116.

Crisp, D., et al. (2004), The orbiting carbon observatory (OCO) mission, *Adv. Space Res.*, *34*, 700–709.

Frankenberg, C., et al. (2015), The Orbiting Carbon Observatory (OCO-2): Spectrometer performance evaluation using pre-launch direct sun measurements, *Atmos. Meas. Tech.*, *8*, 301–313.

Fraser, R. S., and Y. J. Kaufman (1985), The relative importance of aerosol scattering and absorption in remote-sensing, *IEEE Trans. Geosci. Remote*, *23*(5), 625–633.

Goody, R. M., and Y. L. Yung (1989), *Atmospheric Radiation: Theoretical Basis*, 2nd ed., Oxford Univ. Press, Oxford, U. K.

Houweling, S., W. Hartmann, I. Aben, H. Schrijver, J. Skidmore, G. J. Roelofs, and F. M. Breon (2005), Evidence of systematic errors in SCIAMACHY-observed CO_2 due to aerosols, *Atmos. Chem. Phys.*, *5*, 3003–3013.

Kahn, R. A., B. J. Gaitley, J. V. Martonchik, D. J. Diner, K. A. Crean, and B. Holben (2005), Multiangle Imaging Spectroradiometer (MISR) global aerosol optical depth validation based on 2 years of coincident Aerosol Robotic Network (AERONET) observations, *J. Geophys. Res.*, *110*, D10S04, doi:10.1029/2004JD004706.

Kalnay, E., et al. (1996), The NCEP/NCAR 40-year reanalysis project, *Bull. Am. Meteorol. Soc.*, *77*, 437–471.

Kuang, Z. M., J. Margolis, G. Toon, D. Crisp, and Y. Yung (2002), Spaceborne measurements of atmospheric CO_2 by high-resolution NIR spectrometry of reflected sunlight: An introductory study, *Geophys. Res. Lett.*, *29*(15), 1716, doi:10.1029/2001GL014298.

Liang, S. L., H. L. Fang, M. Z. Chen, C. J. Shuey, C. Walthall, C. Daughtry, J. Morisette, C. Schaaf, and A. Strahler (2002), Validating MODIS land surface reflectance and albedo products: Methods and preliminary results, *Remote Sens. Environ.*, *83*, 149–162.

Mandrake, L., C. Frankenberg, C. W. O'Dell, G. Osterman, P. Wennberg, and D. Wunch (2013), Semi-autonomous sounding selection for OCO-2, *Atmos. Meas. Tech.*, *6*, 2851–2864.

Miller, C. E., et al. (2007), Precision requirements for space-based X-CO_2 data, *J. Geophys. Res.*, *112*, D10314, doi:10.1029/2006JD007659.

O'Dell, C. W., et al. (2012), The ACOS CO_2 retrieval algorithm—Part 1: Description and validation against synthetic observations, *Atmos. Meas. Tech.*, *5*, 99–121.

Oshchepkov, S., A. Bril, and T. Yokota (2008), PPDF-based method to account for atmospheric light scattering in observations of carbon dioxide from space, *J. Geophys. Res.*, *113*, D23210, doi:10.1029/2008JD010061.

Ponte, R. M., and J. Dorandeu (2003), Uncertainties in ECMWF surface pressure fields over the ocean in relation to sea level analysis and Modeling, *J. Atmos. Oceanic Technol.*, *20*, 301–307.

Rayner, P. J., and D. M. O'Brien (2001), The utility of remotely sensed CO_2 concentration data in surface source inversions, *Geophys. Res. Lett.*, *28*, 175–178.

Remer, L. A., et al. (2008), Global aerosol climatology from the MODIS satellite sensors, *J. Geophys. Res.*, *113*, D14S07, doi:10.1029/2007JD009661.

Rodgers, C. D. (2000), *Inverse Methods for Atmospheric Sounding: Theory and Practice*, World Sci., Singapore.

Rothman, L. S., et al. (2009), The HITRAN 2008 molecular spectroscopic database, *J. Quant. Spectrosc. Radiat. Transfer*, *110*, 533–572.

Sanghavi, S., J. V. Martonchik, J. Landgraf, and U. Platt (2012), Retrieval of the optical depth and vertical distribution of particulate scatterers in the atmosphere using O-2 A- and B-band SCIAMACHY observations over Kanpur: A case study, *Atmos. Meas. Tech.*, *5*(5), 1099–1119.

Sayer, A. M., N. C. Hsu, C. Bettenhausen, and M. J. Jeong (2013), Validation and uncertainty estimates for MODIS Collection 6 "Deep Blue" aerosol data, *J. Geophys. Res. Atmos.*, *118*, 7864–7872.

Seidel, F. C., and C. Popp (2012), Critical surface albedo and its implications to aerosol remote sensing, *Atmos. Meas. Tech.*, *5*, 1653–1665.

Spurr, R., and V. Natraj (2011), A linearized two-stream radiative transfer code for fast approximation of multiple-scatter fields, *J. Quant. Spectros. Radiat. Transfer*, *112*, 2630–2637.

Uchino, O., et al. (2012), Influence of aerosols and thin cirrus clouds on the GOSAT-observed CO_2: A case study over Tsukuba, *Atmos. Chem. Phys.*, *12*, 3393–3404.

Uppala, S. M., et al. (2005), The ERA-40 re-analysis, *Q. J. R. Meteorol. Soc.*, *131*, 2961–3012.

Wells, K. C., J. V. Martins, L. A. Remer, S. M. Kreidenweis, and G. L. Stephens (2012), Critical reflectance derived from MODIS: Application for the retrieval of aerosol absorption over desert regions, *J. Geophys. Res.*, *117*, D03202, doi:10.1029/2011JD016891.

Wiscombe, W. J. (1977), Delta-M method—Rapid yet accurate radiative flux calculations for strongly asymmetric phase functions, *J. Atmos. Sci.*, *34*, 1408–1422.

Xi, X., V. Natraj, R. L. Shia, M. Luo, Q. Zhang, S. Newman, S. P. Sander, and Y. L. Yung (2015), Simulated retrievals for the remote sensing of CO_2, CH_4, CO, and H_2O from geostationary orbit, *Atmos. Meas. Tech.*, *8*, 4817–4830.

Zhang, Q., V. Natraj, K. F. Li, R. L. Shia, D. J. Fu, T. J. Pongetti, S. P. Sander, C. M. Roehl, and Y. L. Yung (2015), Accounting for aerosol scattering in the CLARS retrieval of column averaged CO_2 mixing ratios, *J. Geophys. Res. Atmos.*, *120*, 7205–7218, doi:10.1002/2015JD023499.